Doc Ophthalmol
DOI 10.1007/s10633-016-9524-3

ORIGINAL RESEARCH ARTICLE

Is multifocal electroretinography an early predictor of glaucoma?

Haydar Gölemez · Nilgün Yıldırım · Ahmet Özer

Received: 3 October 2015 / Accepted: 6 January 2016

Abstract

Purpose To investigate the potential use of mfERG as an objective functional test that can express inner and outer retinal changes during the early stages of glaucoma.

Methods One hundred and twenty-six eyes of 126 patients were included. There were 30 healthy (Group 1), 28 glaucoma suspect (Group 2), 48 early glaucoma (Group 3), and 20 advanced glaucoma cases (Group 4). After complete ophthalmic examination, Humphrey visual field analysis and mfERG were performed. These examinations were performed three times at 6-month intervals, and only the last examination results were used for the analysis. Visual fields global indices and mfERG implicit time and amplitudes were evaluated and analyzed by ring system (central 5°, 5°–10°, 10°–15° and >15°). One-way ANOVA and ROC curve analysis were used for statistical analysis.

Results There was no statistically (one-way ANOVA) significant differences in patient age between groups ($p = 0.126$). For all rings, we detected statistically significant differences for the mean implicit time (latency) of the N1, P1, and N2 components between the advanced glaucoma and control subjects and between the advanced glaucoma and glaucoma suspects. The N2 amplitudes were significantly decreased in all rings in the advanced glaucoma patients when compared with control subjects. The N2 amplitude was significantly different between healthy subjects (Group 1) and early glaucoma subjects (Group 3) in the central 2° and 2°–5° rings. We used MedClac ROC curve analysis to identify the best parameters for discriminating between control subjects (Group 1) and early glaucoma patients (Group 3). The N2 implicit time for the central 2° ring ($p < 0.0001$), N2 amplitude for the central 2° ring ($p = 0.0001$), P1 implicit time for the 2°–5° ring ($p = 0.0001$), N2 implicit time for the 2°–5° ring ($p = 0.0003$), and N2 amplitude for the 2°–5° ring ($p = 0.001$) had ≥0.7 AUC values and were the best parameters in the ROC curve analyses that included the VFA parameters

Conclusion Alterations of amplitudes and implicit times of N2 response in the central area may be able to detect glaucoma earlier than VFA. In addition, with progression to advanced glaucoma these changes can be significant in all retinal areas. Although implicit times of all mfERG components are significantly delayed in glaucoma, both delayed implicit time and decreased amplitude of N2 wave in the central area are effective predictors in early glaucoma diagnosis.

H. Gölemez (✉)
Department of Ophthalmology, Eskisehir State Hospital, Yenidoğan Mh. Şehit Serkan Özaydın Sokak No:1, 26060 Odunpazarı, Eskisehir, Turkey
e-mail: hgolemez@gmail.com

N. Yıldırım · A. Özer
Department of Ophthalmology, Eskisehir Osmangazi University, Meselik, Eskisehir, Turkey

Published online: 20 January 2016

Keywords Glaucoma · Multifocal electroretinography · Ring analysis · Photopic negative response · N2 wave · Amplitude · Latency · Implicit time · Humphrey perimetry

Introduction

Glaucoma is a pathological process that results in the loss of retinal ganglion cells and axons [1] and is a major cause of blindness worldwide [2]. Glaucomatous damage is often evaluated by optic disk examination, retinal nerve fiber layer examination, and a visual field test. However, early detection of initial ganglion cell damage is not possible using the current standard visual field tests [3, 4]. Several studies have shown that the structural damage that occurs before the visual field defects can be detected in early glaucoma patients [5–7]. Such damage must involve at least 40 % of the retinal ganglion cell axons to be detectable by Humphrey perimetry. Glaucoma detection by short-wavelength automated perimetry (SWAP), frequency-doubling technology (FDT) perimetry, or high-pass resolution perimetry (HRP) is more sensitive to early defects and disease progression [8–12]. Unfortunately, these methods are limited to detecting damage involving $\sim$15 % retinal ganglion cell axons. Although optic nerve topography and retinal nerve fiber layer analyzers can be used to detect structural damage, here we aimed to develop an objective test able to detect early functional damage of ganglion cells.

Techniques to objectively measure visual functions (e.g., electrophysiological tests) have been successfully used for early detection of glaucoma [11–13]. An animal study found that electrophysiological changes in the flash electroretinography (flash ERG) of mice following laser-induced ocular hypertension (OHT) can be detected after 24–48 h, and these changes persisted throughout the study [14]. Such experimental glaucoma studies have also reported immunohistochemically or morphologically identified RGC death within 3–8 days [14, 15]. These findings demonstrate that electrophysiological deterioration starts before (or at the same time as) retinal ganglion cell (RGC) death. Compared to perimetry approaches, pattern electroretinogram (PERG) seems a viable alternative for distinguishing between glaucoma and normal eyes [12]. This is interesting because PERG reports the sum of the central retinal response, which is usually preserved in glaucoma until the final disease phase [11, 13]. PERG studies have also shown that the ganglion cells in the central retinal area may be affected in early glaucoma [16–19]. Thus, PERG can detect early losses that cannot be determined by other routine perimeter methods.

The multifocal electroretinography (mfERG) technique, developed by Sutter et al., can record large numbers of localized retinal responses within a few minutes [20, 21]. Compared to the PERG test, the mfERG technique gives precise information about the electrical activity of the central and peripheral retina [22]. In addition, generalized defects such as retinitis pigmentosa [23] and optic atrophy [24] and localized defects such as retinal detachment [25] can be detected by mfERG. Although mfERG is most often used to detect damage of photoreceptor cells, several studies have also employed this technique to investigate glaucoma [26–28]. Other studies have used mfERG to detect the altered dendritic processes of ON-rod bipolar and horizontal cells and cone density loss in glaucoma [29–31]. Here we investigate the potential use of mfERG as an objective functional test that can express inner and outer retinal changes during the early stages of glaucoma.

Methods

Subjects

Subjects were divided into four groups according to their disease state (healthy control, glaucoma suspect, early glaucoma, and advanced glaucoma). Thirty eyes of 30 normal subjects (mean age: 53.28 $\pm$ 10.76 years) were tested as control subjects (Group 1). The glaucoma suspect group (Group 2) consisted of 28 eyes of 28 patients (mean age: 55.06 $\pm$ 8.53 years). Sixty-eight eyes of 68 glaucoma patients (mean age: 55.22 $\pm$ 10.19 years) were analyzed. There was no statistically (one-way ANOVA) significant differences in patient age between groups ($p = 0.126$). Subjects with glaucoma diagnosis were divided into two subgroups according to the Hodapp–Parrish–Anderson glaucoma grading scale. Patients with relatively slight damage were grouped as early glaucoma (Group 3) ($n = 48$) and those with severe damage as advanced

glaucoma (Group 4) ($n = 20$). Early glaucoma subjects were in Stage 1 and the advanced subjects in Stage 2 or higher. Glaucoma suspects were selected from patients with an IOP values of >21 mmHg detected on at least two occasions, with suspected optic disk changes in routine ophthalmic examination or with glaucoma family story. These subjects had no identified glaucomatous damage in the visual field and HRT II tests. All glaucoma patients were diagnosed as POAG and receiving medical therapy without a previous surgery history. In addition, all other control and glaucoma suspect subjects were open angled. The patients had clear medias and did not have any other ocular or systemic diseases. Their corrected visual acuities were >20/20. Refractive errors were within ±5.0 diopters.

Recordings

The visual field analyses (VFA) of subjects were evaluated using a Humphrey perimetry system Model 750 (Humphrey Instruments, San Leandro, Calif, USA). During the visual field test, the Swedish interactive thresholding algorithm (SITA) standard strategy and the central 30–2 threshold test were used. Tests with more than 20 % fixation loses and more than 30 % false-positive or false-negative response were repeated [32] Patients that were unable to adapt to the tests were excluded. The pattern deviation map was divided in four rings [5° (central); 5°–10°, 10°–15°, and ≥15°] (Fig. 1). The average pattern deviation values were calculated for each ring.

A Metrovision MonElec 2 electrophysiology system (Metrovision, Perenchies, France) was used to record the mfERGs. Patients were left in a dimly lit room 20 min for adaptation after pupil dilatation with a tropicamide. Local anesthetic was applied to one eye before placing a single-use unipolar gold-based contact lens active electrode (ERG Jet, Metrovision, Perenchies, France) to obtain highest signal-to-noise ratio [33]. The other eye was then occluded. A neutral electrode (cupula) was placed on the forehead and grounding electrodes (ear clips) were attached to the front of the ear. If the patient needed spherical correction, adjustable glasses were used during the test. The test was performed from 30 cm distance, and the subject was installed on a chin rest. Frequency of m-sequence was set at 17 Hz. Frame rate of stimulator was 120 Hz. Stimulus was sent from a luminance-controlled LED monitor against a 30-cd/m^2 ground lighting. For bright, dark, and average hexagonal stimulus, luminance was set to 200, <5, and 101 cd/m^2, respectively. The stimulus contrast was >95 %. The device automatically evaluated signals from each of the retinal areas during the test, with a maximum of 200 corrupt signals and approximately 10,000 signals being obtained by the end of the test. Fixation was controlled using a built-in near-infrared camera during the test. If there were more than 30/150 fixation loses, the test was stopped and repeated. Patients who could not adapt to the test was excluded. An average wave consisting of N1, P1, and N2 components was obtained for each of the 91 retinal areas. The amplitude and latency (implicit time) of these three components were analyzed using first-order kernels. Thereafter, as seen in the visual field test, the N1, P1, and N2 components, amplitude, and latency were automatically computer-calculated for each ring area. The central 5° section was divided into 2° and 2°–5° rings automatically by MonElec 2 electrophysiology system (Fig. 2).

Both the visual field and mfERG recordings were performed at least three times, and the third examination was used for statistical analysis. Cases with any missing data in both of the tests were excluded.

Statistical analysis

One-way ANOVA (IBM SPSS statistics 21 software package) was used to assess the differences between groups. Parameters were checked normality separately for each group. Tukey's HSD was used as post hoc test. ROC curve analysis (MedCalc version 15) was used to identify the best parameters to distinguish between the healthy and early glaucoma subjects (Group 1 vs Group 3).

Results

Statistically different VFA and MfERG values between groups

The parameters acquired by VFA were compared by one-way ANOVA, and no statistically significant differences were identified between the control (Group 1) and glaucoma suspects (Group 2) or between the control (Group 1) and early glaucoma patients (Group 3). However, the advanced glaucoma group (Group 4) was statically different from all of the other groups for

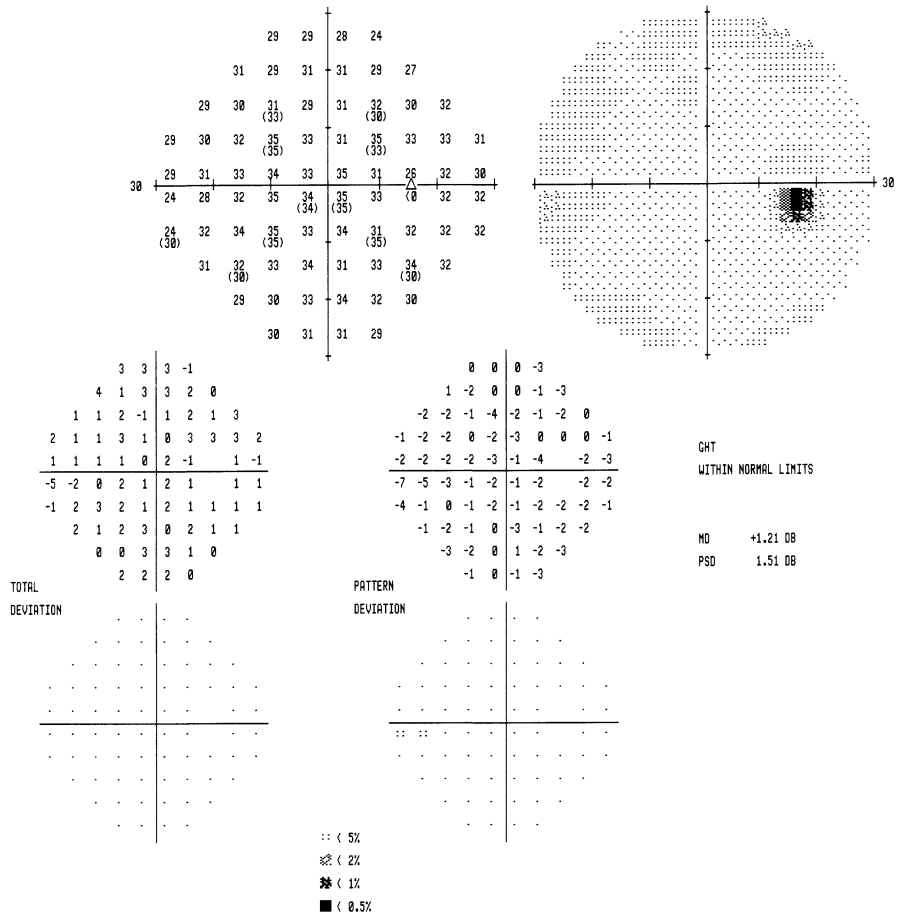

Fig. 1 Rings shown in VFA pattern deviation map. The pattern deviation map was divided in four rings [5° (central); 5°–10°, 10°–15° and ≥15°]

the global MD, global PSD, and pattern deviation mean values at the central 5°, 5°–10°, 10°–15°, and ≥15° rings. The global mean deviation values by the visual field test were −1.58, −2.46, −2.62, and −11.8 dB for control subjects, glaucoma suspects, and early and advanced glaucoma patients, respectively. The global pattern standard deviations acquired by the visual field test were 1.84, 2.18, 2.25, and 8.77 dB for control subjects, glaucoma suspects, and early and advanced glaucoma patients, respectively. The mean values of pattern deviation acquired by ring analysis with VFA are shown in Table 1, and the mean differences between groups determined by one-way ANOVA are shown in Table 2.

For all rings, we detected statistically significant differences for the mean implicit time (latency) of the N1, P1, and N2 components between the advanced glaucoma and control subjects and between the advanced glaucoma and glaucoma suspects. The N2 amplitudes were significantly decreased in all rings in the advanced glaucoma patients when compared with control subjects. The change in N2 amplitude was statically significant between Group 2 and 4 and between Group 3 and 4, especially in the central 2° ring. The N2 amplitude significantly different between Group 1 and 3 in the central 2° and 2°–5° rings. A P1 amplitude decrease was seen in central 2° ring of the advanced glaucoma patients compared with the control subjects, except for the N2 amplitude changes. MfERG amplitude and latency mean values are shown in Table 3, and the differences between groups determined by one-way ANOVA are shown in Table 4.

We used MedClac ROC curve analysis to identify the best parameters for discriminating between control subjects and early glaucoma patients. AUC of ROC curve analysis, which is interpreted as the average value of sensitivity for all possible values of

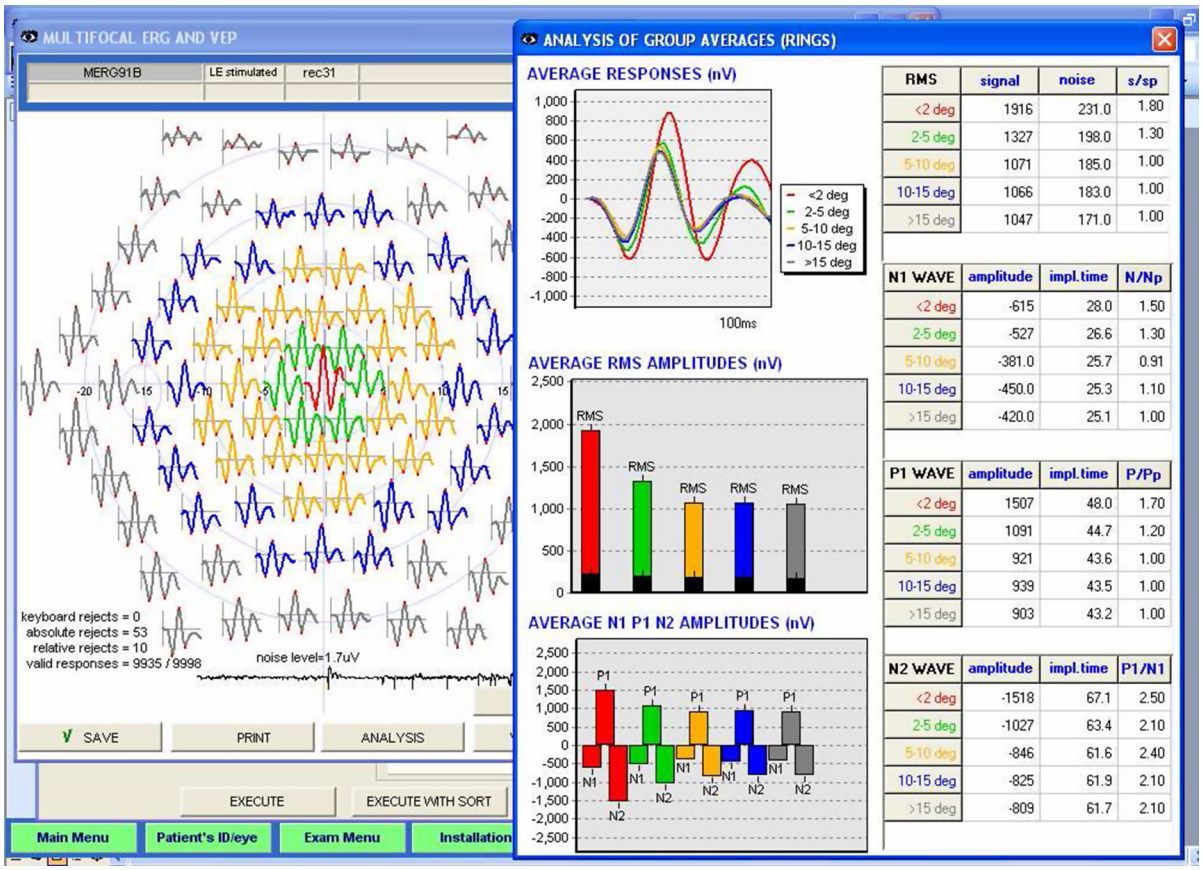

Fig. 2 Ring analysis in the mfERG test. MfERG map was divided in five rings (<2°, 2°–5°, 5°–10°, 10°–15° and ≥15°)

Table 1 Mean values of global parameters and pattern deviations in ring analysis with VFA

	Group 1 (mean ± SD)	Group 2 (mean ± SD)	Group 3 (mean ± SD)	Group 4 (mean ± SD)
Humphrey global MD	−1.58 ± 1.28	−2.46 ± 1.89	−2.62 ± 1.78	−11.82 ± 5.38
Humphrey global PSD	1.84 ± 0.34	2.18 ± 0.66	2.25 ± 0.69	8.77 ± 3.71
Mean pattern deviation of central 5°	−2.20 ± 0.84	−2.33 ± 0.96	−2.19 ± 1.22	−3.90 ± 5.14
Mean pattern deviation of 5°–10°	−2.13 ± 0.68	−2.17 ± 0.76	−2.17 ± 0.88	−6.44 ± 4.85
Mean pattern deviation of 10°–15°	−1.55 ± .61	−1.77 ± .64	−1.80 ± .74	−6.43 ± 3.80
Mean pattern deviation of >15°	−1.19 ± .63	−1.65 ± 1.32	−1.84 ± 1.26	−7.97 ± 4.91

specificity, is a measure of the overall performance of a diagnostic test [34, 35]. According to MedClac ROC curve analysis, if the p value is small (i.e., $p < 0.05$), then it can be concluded that the area under the ROC curve (AUC) is significantly different from 0.5 and that, therefore, there is evidence that the test can distinguish between the two groups. Subjects were grouped as control (Group 1) and early glaucoma (Group 3). The N2 implicit time for the central 2° ring ($p < 0.0001$), N2 amplitude for the central 2° ring ($p = 0.0001$), P1 implicit time for the 2°–5° ring ($p = 0.0001$), N2 implicit time for the 2°–5° ring ($p = 0.0003$), and N2 amplitude for the 2°–5° ring ($p = 0.001$) were the best parameters in the ROC

Table 2 Mean differences between groups as determined by one-way ANOVA

	Group 1 versus Group 2	Group 1 versus Group 3	Group 1 versus Group 4	Group 2 versus Group 3	Group 2 versus Group 4	Group 3 versus Group 4
Humphrey global MD	–	–	*	–	*	*
Humphrey global PSD	–	–	*	–	*	*
Mean pattern deviation of central 5° section	–	–	*	–	–	*
Mean pattern deviation of 5°–10° section	–	–	*	–	*	*
Mean pattern deviation of 10°–15° section	–	–	*	–	*	*
Mean pattern deviation of >15° section	–	–	*	–	*	*

* The mean difference is significant at the 0.05 level

curve analyses that included the VFA parameters (Table 5). These five parameters had more reasonable results with ≥0.7 AUC values.

Discussion

Here we compared both early-stage and advanced glaucoma with normal subjects and glaucoma suspects. We aimed to show a transition from suspected cases to glaucoma and to determine whether mfERG would be useful in early diagnosis of glaucoma. In advanced glaucoma, the implicit times of the mfERG components are usually affected and delayed. This condition is expected in severe ganglion cell loss and when the retinal nerve fiber layer affected. In our study, the implicit times of all components (N1, P1 and N2) of the mfERG waveform were delayed in advanced glaucoma subjects in all retinal areas. The implicit time changes in the central area were more remarkable than in the periphery. Using mfERG, Parisi et al. [36] found a significant decrease in the N1–P1 amplitudes and an increase in the P1 implicit time in the central macular area (but no other significant differences) of open-angle glaucoma (OAG) patients compared with controls, with the authors suggesting a macular functional impairment in glaucoma patients that can be mostly accounted for by contributions from preganglionic elements (photoreceptors and OFF bipolar cells). The same differences between patients and controls were detected in our study. In addition, we detected an N2 amplitude decline in the central 5° ring (for early glaucoma) and in all rings (for advanced glaucoma), compared to controls. Hasegawa et al. [26] suggested that the peak implicit times (but not the amplitudes) of the mfERG increase as the glaucomatous visual field deteriorates. Because their study used quadrant analysis, no central or periphery comparisons have been made; however, no significant differences in amplitudes (including N2) were detected. The N1 response of mfERG includes cellular contributions from the same components as the a-wave of the full-field cone ERG, and the P1 response includes contributions from the components of the cone b-wave and oscillatory potentials [33]. In PERG there is an early negative wave at about 30 ms, a positive wave at about 50 ms (P50), and a later negativity at about 95 ms, known as N95. N95 appears to reflect activity from the ganglion cell layer. N95 shows greater variation in amplitude with spatial frequency and is more affected in diseases of the optic nerve [37]. P50, however, is altered in a number of diseases that primarily affect the outer retina [37]. A ratio of P50 and N95 has been suggested as useful in discriminating a number of diseases that affect the optic nerve [37–40].

Thereafter Viswanathan et al. [27] discovered photopic negative response (PhNR) and investigated PhNR of the macaque electroretinogram in experimental glaucoma. They suggested that PhNR is most likely arises from retinal ganglion cells and their axons, but its slow timing raises the possibility that it could be mediated by glia. And they concluded that regardless of the mechanism of its generation, the

Table 3 Mean values of amplitude and implicit time with ring analyses with mfERG in groups

	Group 1	Group 2	Group 3	Group 4
N1 amplitude				
Central 2°	−76,797	−75,607	−76,102	−65,484
2°–5°	−470,355	−499,500	−462,551	−445,053
5°–10°	−392,065	−377,000	−378,449	−346,789
10°–15°	−395,387	−412,133	−406,204	−346,474
>15°	−432,548	−456,600	−439,755	−381,368
N1 implicit time				
Central 2°	26,755	27,297	27,435	30,716
2°–5°	25,881	26,253	26,965	27,332
5°–10°	24,955	25,507	25,896	26,716
10°–15°	25,168	25,617	26,084	27,047
>15°	25,239	25,743	26,151	27,189
P1 amplitude				
Central 2°	170,052	160,277	148,994	134,911
2°–5°	105,658	99,873	95,108	92,632
5°–10°	847,000	777,733	786,469	719,316
10°–15°	857,194	799,233	804,694	735,368
>15°	949,258	887,800	901,408	789,421
P1 implicit time				
Central 2°	49,319	49,943	50,992	52,884
2°–5°	44,865	45,297	45,988	46,858
5°–10°	43,265	43,833	44,276	45,063
10°–15°	4346	4386	4440	4542
>15°	43,361	43,807	44,373	45,437
N2 amplitude				
Central 2°	−178,284	−159,483	−147,259	−121,337
2°–5°	−98,597	−86,023	−84,357	−77,579
5°–10°	−730,129	−660,867	−660,878	−606,053
10°–15°	−750,097	−633,667	−656,857	−605,684
>15°	−855,000	−725,500	−756,592	−650,105
N2 implicit time				
Central 2°	6852	6952	7063	7172
2°–5°	6349	6395	6472	6645
5°–10°	61,858	62,183	62,563	63,132
10°–15°	61,926	61,927	62,616	63,289
>15°	61,571	61,680	62,357	63,126

PhNR holds promise as an indicator of retinal function in early glaucomatous optic neuropathy.

Colotto et al. [41] investigated the photopic negative response (PhNR) in human glaucoma and noticed the inner retinal origin for PhNR. They showed reduced PhNR but normal a- and b-wave amplitudes when compared control subjects with OAG patients. Also in patients with OHT, PhNR and a- and b-wave amplitudes did not differ from control values. Similar to that found in monkeys with experimentally induced glaucoma, the PhNR was selectively altered in human glaucoma. They suggested that PhNR may be directly or indirectly related to ganglion cell activity, because the PERG N95 is thought to specifically reflect the functional integrity of these neurons [42, 43]. Colotto et al. [41] concluded that the correlation between

Table 4 Parameters of the MfERG compared between groups with one-way ANOVA

Ring	Group 1 versus Group 2	Group 1 versus Group 3	Group 1 versus Group 4	Group 2 versus Group 3	Group 2 versus Group 4	Group 3 versus Group 4
N1 amplitude						
Central 2°	–	–	–	–	–	–
2°–5°	–	–	–	–	–	–
5°–10°	–	–	–	–	–	–
10°–15°	–	–	–	–	–	–
>15°	–	–	–	–	–	–
N1 implicit time						
Central 2°	–	–	*	–	*	*
2°–5°	–	*	*	–	–	–
5°–10°	–	*	*	–	*	–
10°–15°	–	*	*	–	*	*
>15°	–	*	*	–	*	–
P1 amplitude						
Central 2°	–	–	*	–	–	–
2°–5°	–	–	–	–	–	–
5°–10°	–	–	–	–	–	–
10°–15°	–	–	–	–	–	–
>15°	–	–	–	–	–	–
P1 implicit time						
Central 2°	–	*	*	–	*	*
2°–5°	–	*	*	–	*	–
5°–10°	–	*	*	–	*	–
10°–15°	–	*	*	–	*	*
>15°	–	*	*	–	*	*
N2 amplitude						
Central 2°	–	*	*	–	*	*
2°–5°	*	*	*	–	–	–
5°–10°	–	–	*	–	–	–
10°–15°	–	–	*	–	–	–
>15°	–	–	*	–	–	–
N2 implicit time						
Central 2°	–	*	*	–	*	–
2°–5°	–	*	*	–	*	*
5°–10°	–	–	*	–	–	–
10 –15°	–	–	*	–	*	–
>15°	–	–	*	–	*	–

* The mean difference is significant at the 0.05 level

PhNR losses and clinical parameter abnormalities suggests that this component depends on inner retina integrity and may be of clinical value for detecting glaucomatous damage. Wilsey et al. [44] reviewed glaucoma and electroretinography. Although electrophysiological measurements including mfERG are all

Table 5 ROC analysis of mfERG and VFA parameters

Variable	AUC	SE	95 % CI	p value (area = 0.5)	Sensitivity	Specificity
N2 impl. time 2°	0.762	0.0548	0.654–0.850	<0.0001	46.94	93.55
N2 amplitude 2°	0.728	0.0592	0.617–0.822	0.0001	75.51	61.29
P1 impl. time 2°–5°	0.725	0.0568	0.614–0.819	0.0001	65.31	80.65
N2 impl. time 2°–5°	0.709	0.0579	0.597–0.805	0.0003	87.76	48.39
N2 amplitude 2°–5°	0.703	0.0621	0.591–0.800	0.0010	87.76	48.39
P1 impl. time 5°–10°	0.699	0.0581	0.586–0.797	0.0006	61.22	80.65
P1 impl. time 2°	0.697	0.0583	0.585–0.795	0.0007	44.90	93.55
N1 impl. time 2°–5°	0.696	0.0580	0.583–0.794	0.0007	42.86	93.55
N1 impl. time 5°–10°	0.691	0.0585	0.578–0.790	0.0011	38.78	93.55
Humphrey global PSD	0.691	0.0590	0.578–0.790	0.0012	44.90	90.32
N2 impl. time 15°	0.680	0.0605	0.566–0.780	0.0029	55.10	77.42
Mean pattern deviation (>15°)	0.679	0.0603	0.566–0.779	0.0029	51.02	80.65
P1 impl. time 10°–15°	0.674	0.0602	0.560–0.774	0.0039	61.22	80.65
P1 impl. time 15°	0.673	0.0596	0.559–0.774	0.0038	53.06	80.65
N1 impl. time 10°–15°	0.672	0.0597	0.558–0.773	0.0039	53.06	80.65
Humphrey global MD	0.657	0.0607	0.543–0.760	0.0096	32.65	96.77
N2 impl. time 10°–15°	0.652	0.0632	0.537–0.755	0.0162	46.94	80.65
P1 amplitude 2°–5°	0.648	0.0631	0.533–0.751	0.0192	51.02	77.42
P1 amplitude 2°	0.648	0.0637	0.534–0.752	0.0198	48.98	83.87
N2 impl. time 5°–10°	0.645	0.0619	0.531–0.749	0.0188	46.94	80.65
N2 amplitude 10°–15°	0.644	0.0636	0.529–0.748	0.0234	61.22	67.74
N1 impl. time 15°	0.636	0.0615	0.521–0.741	0.0270	38.78	96.77
N2 amplitude 5°–10°	0.635	0.0648	0.519–0.740	0.0378	59.18	67.74

sensitive to glaucomatous damage they suggested that PERG and PhNR responses obtained from the central macula are capable of detecting early-stage, reversible glaucomatous dysfunction. In a recent experimental study, ElGohary et al. [45] used VEP and ERG in glaucomatous rabbit model and described PhNR and VEP good additional tools in early diagnosis of glaucoma. Using mfERG, OCT, and visual field analysis, Ledolter et al. [46] showed a statistically significant correlation of mfERG with perimetric sensitivity measured in linear units and with structural macular changes detected with time-domain OCT.

Recently, Kaneko et al. [28] used mfERG in glaucoma patients and described the N2 wave as PhNR. The N2 response density was proportionately reduced in the central area with the severity of glaucoma. Similar to our findings, Kaneko et al. proposed that the reduction in the N2 amplitude is significant in the early stage of glaucoma and correlated with the perimetry and thickness of the ganglion cell complex. Kaneko et al. concluded that, in glaucoma, the N2 component is affected in the central area. Similar to Kaneko et al. [28] another recent study of Kato et al. [47] found that N2 amplitude was significantly smaller in the glaucomatous eyes than the normal eyes in all retinal areas. Also there was a significant correlation between the N2 amplitude with HFA and RNFL thickness. Authors concluded that results of study indicates that the activity of the retinal ganglion cells contribute to the amplitude of the N2 of the mfERGs and thus can be used as an objective monitor of retinal ganglion cell function. As in N2 amplitude changes, Todorova et al. [48] showed delay of the N2 latency in POAG, especially in with high-tension glaucoma patients using long-duration white stimulus.

Until recently, the N2 component of the mfERG seemed to be an insignificant parameter for glaucoma

detection. However, our study and other recent studies [28, 47] have shown that the late onset negative response of mfERG is useful for detecting glaucomatous damage. Our ROC analysis found that both the decreased amplitude and delayed implicit time of the N2 response in the central retinal area, especially in the 5° zone, are valuable (and better than all other mfERG and HFA parameters) in discriminating glaucoma patients from normal subjects (Table 5). During progression of glaucoma to the advanced stage, N2 amplitude depression becomes significant in all rings (Table 4). The decline in N2 amplitude was the only alteration detected in the amplitudes of the mfERG waveform, except for the P1 amplitude difference between advanced glaucoma and normal subjects (Table 4).

In conclusion, alterations of amplitudes and implicit times of N2 response in the central area may be able to detect glaucoma earlier than VFA. In addition, with progression to advanced glaucoma, these changes can be significant in all retinal areas. Although implicit times of all mfERG components are significantly delayed in glaucoma, both delayed implicit time and decreased amplitude of N2 wave in the central area are effective predictors in early glaucoma diagnosis. However, mfERG is a difficult test to be used in routine practice and requires experience and laboratory-specific standardization.

Funding No funding was received for this research.

Compliance with ethical standards

Conflict of interest All authors certify that they have no affiliations with or involvement in any organization or entity with any financial interest (such as honoraria; educational grants; participation in speakers' bureaus; membership, employment, consultancies, stock ownership, or other equity interest; and expert testimony or patent-licensing arrangements), or non-financial interest (such as personal or professional relationships, affiliations, knowledge or beliefs) in the subject matter or materials discussed in this manuscript.

Ethical approval All procedures performed in studies involving human participants were in accordance with the ethical standards of the institutional and/or national research committee and with the 1964 Declaration of Helsinki and its later amendments or comparable ethical standards.

Informed consent Informed consent was obtained from all individual participants included in the study.

References

1. Kim T, Park U, Park KH, Kim DM (2007) Ability of stratus OCT to identify localized retinal nerve fiber layer defects in patients with normal standard automated perimetry results. Investig Ophthalmol Vis Sci 48:1635–1641
2. Quigley HA (1996) Number of people with glaucoma worldwide. Br J Ophthalmol 80:389–393
3. Quigley HA, Dunkelberger GR, Green WR (1989) Retinal ganglion cell atrophy correlated with automated perimetry in human eyes with glaucoma. Am J Ophthalmol 107:453–464
4. Harwerth RS, Carter-Dawson L, Shen F, Smith EL 3rd, Crawford ML (1999) Ganglion cell losses underlying visual field defects from experimental glaucoma. Investig Ophthalmol Vis Sci 40:2242–2250
5. Katz J, Sommer A, Gaasterland DE, Anderson DR (1991) Comparison of analytic algorithms for detecting glaucomatous visual field loss. Arch Ophthalmol 109:1684–1689
6. Tuulonen A, Lehtola J, Airaksinen PJ (1993) Nerve fiber layer defects with normal visual fields: do normal optic disc and normal visual field indicate absence of glaucomatous abnormality? Ophthalmol 100:587–597
7. Quigley HA, Katz J, Derick RJ, Gilbert D, Sommer A (1992) An evaluation of optic disc and nerve fiber layer examinations in monitoring progression of early glaucoma damage. Ophthalmology 99:19–28
8. Sample PA, Taylor JD, Martinez GA, Lusky M, Weinreb RN (1993) Short-wavelength color visual fields in glaucoma suspects at risk. Am J Ophthalmol 115:225–233
9. Wall M, Ketoff KM (1995) Random dot motion perimetry in patients with glaucoma and in normal subjects. Am J Ophthalmol 120:587–596
10. Johnson CA, Samuels SJ (1997) Screening for glaucomatous visual field loss with frequency-doubling perimetry. Investig Ophthalmol Vis Sci 38:413–425
11. Chauhan BC, House PH, McCormick TA, LeBlanc RP (1999) Comparison of conventional and high pass resolution perimetry in a prospective study of patients with glaucoma and healthy controls. Arch Ophthalmol 117:24–33
12. Johnson CA, Adams AJ, Casson EJ, Brandt BD (1993) Progression of early glaucomatous visual field loss as detected by blue-on-yellow and standard white-on-white automated perimetry. Arch Ophthalmol 111:651–656
13. Korth M (1997) The value of electrophysiological testing in glaucomatous diseases. J Glaucoma 6:331–343
14. Salinas-Navarro M, Alarcón-Martínez L, Valiente-Soriano FJ, Ortín-Martínez A, Jiménez-López M, Avilés-Trigueros M, Villegas-Pérez MP, de la Villa P, Vidal-Sanz M (2009) Functional and morphological effects of laser-induced ocular hypertension in retinas of adult albino swiss mice. Mol Vis 15:2578–2598
15. Wang X, Ng YK, Tay SS (2005) Factors contributing to neuronal degeneration in retinas of experimental glaucomatous rats. J Neurosci Res 82:674–689
16. Maffei L, Fiorentini A (1981) Electroretinographic responses to alternating gratings before and after section of the optic nerve. Science 211:953–955

17. Maffei L, Fiorentini A, Bisti S, Hollander H (1985) Pattern ERG in the monkey after section of the optic nerve. Exp Brain Res 59:423–425
18. Marx MS, Podos SM, Bodis-Wollner I, Howard-Williams JR, Siegel MJ, Teitelbaum CS, Maclin EL, Severin C (1986) Flash and pattern electroretinograms in normal and laser-induced glaucomatous primate eyes. Investig Ophthalmol Vis Sci 27:378–386
19. Johnson MA, Drum BA, Ha Quigley, Sanchez RM, Dunkelberger GR (1989) Pattern evoked potentials and optic nerve fiber loss in monocular laser-induced glaucoma. Investig Ophthalmol Vis Sci 30:897–907
20. Sutter EE (1991) The fast m-transform: a fast computation of cross-correlations with binary m-sequences. Soc Ind Appl Math 20:686–694
21. Sutter EE, Tran D (1992) The field topography of ERG components in man I: the photopic luminance response. Vis Res 32:433–466
22. Sutter EE (1992) A deterministic time-domain nonlinear analysis. In: Pinter RB, Nabet B (eds) Nonlinear vision. CRC Press, London, pp 171–220
23. Chan HL, Brown B (1998) Investigation of retinitis pigmentosa using the multifocal electroretinogram. Ophthalmic Physiol Opt 18:335–350
24. Bearse MA Jr, Sutter EE, Smith DN (1995) Ganglion cell components of the human multifocal ERG are abnormal in optic nerve atrophy and glaucoma. Investig Ophthalmol Vis Sci 36(suppl):444
25. Sasoh M, Yoshida S, Kuze M (1998) The multifocal electroretinogram in retinal detachment. Doc Ophthalmol 94:239–252
26. Hasegawa S, Takagi M, Usui T, Abe H (2000) Waveform changes of the first-order multifocal electroretinogram in patients with glaucoma. Investig Ophthalmol Vis Sci 41:1597–1603
27. Viswanathan S, Frishman LJ, Robson JG, Harwerth RS, Smith EL III (1999) The photopic negative response of the macaque electroretinogram: reduction by experimental glaucoma. Investig Ophthalmol Vis Sci 40:1124–1136
28. Kaneko M, Machida S, Hoshi Y, Kurosaka D (2015) Alterations of photopic negative response of multifocal electroretinogram in patients with glaucoma. Curr Eye Res 40:77–86
29. Lei Y, Garrahan N, Hermann B, Becker DL, Hernandez MR, Boulton ME, Morgan JE (2008) Quantification of retinal transneuronal degeneration in human glaucoma: a novel multiphoton-DAPI approach. Investig Ophthalmol Vis Sci 49:1940–1945
30. Panda S, Jonas JB (1992) Decreased photoreceptor count in human eyes with secondary angle-closure glaucoma. Investig Ophthalmol Vis Sci 33:2532–2536
31. Lei Y, Garrahan N, Hermann B, Fautsch MP, Johnson DH, Hernandez MR, Boulton M, Morgan JE (2010) Transretinal degeneration in ageing human retina: a multiphoton microscopy analysis. Br J Ophthalmol 95:727–730
32. Katz J, Sommer A (1990) Screening for glaucomatous visual field loss: the effect of patient reliability. Ophthalmology 97(8):1032–1037
33. Hood DC, Bach M, Brigell M, Keating D, Kondo M, Lyons JS, Marmor MF, McCulloch DL, Palmowski-Wolfe AM, International Society for Clinical Electrophysiology of Vision (2012) ISCEV standard for clinical multifocal electroretinography (mfERG) (2011) edition. Doc Ophthalmol 124:1–13
34. Obuchowski NA (2003) Receiver operating characteristic curves and their use in radiology. Radiology 229:3–8
35. Zhou XH, Obuchowski NA, McClish DK (2002) Statistical methods in diagnostic medicine, 1st edn. Wiley, New York, pp 15–164
36. Parisi V, Ziccardi L, Centofanti M, Tanga L, Gallinaro G, Falsini B, Bucci MG (2012) Macular function in eyes with open-angle glaucoma evaluated by multifocal electroretinogram. Investig Ophthalmol Vis Sci 53:6973–6980
37. Holder GE (1987) The significance of abnormal pattern electroretinography in anterior visual pathway dysfunction. Br J Ophthalmol 71:166
38. Weinstein GW, Arden GB, Hitchings RA et al (1988) The pattern electroretinogram (PERG) in ocular hypertension and glaucoma. Arch Ophthalmol 106:923
39. Odom JV, Holder GE, Feghali JG, Cavender S (1992) Pattern electroretinogram intrasession reliability: a two center comparison. Clin Vis Sci 7:263
40. Holder GE (2001) Pattern electroretinography (PERG) and an integrated approach to visual pathway diagnosis. Prog Retin Eye Res 20:531
41. Colotto A, Falsini B, Salgarello T, Iarossi G, Galan ME, Scullica L (2000) Photopic negative response of the human ERG: losses associated with glaucomatous damage. Investig Ophthalmol Vis Sci 41:2205–2211
42. Holder GE (1987) Significance of abnormal pattern electroretinography in anterior visual pathway dysfunction. Br J Ophthalmol 71:166–171
43. Schuurmans RP, Berninger T (1985) Luminance and contrast responses recorded in man and cat. Doc Ophthalmol 59:187–197
44. Wilsey LJ, Fortune B (2015) Electroretinography in glaucoma diagnosis. Curr Opin Ophthalmol. 2015 Dec 30. [Epub ahead of print]
45. ElGohary AA, Elshazly LH (2015) Photopic negative response in diagnosis of glaucoma: an experimental study in glaucomatous rabbit model. Int J Ophthalmol 8(3):459–464
46. Ledolter AA, Monhart M, Schoetzau A, Todorova MG, Palmowski-Wolfe AM (2015) Structural and functional changes in glaucoma: comparing the two-flash multifocal electroretinogram to optical coherence tomography and visual fields. Doc Ophthalmol 130(3):197–209. doi:10.1007/s10633-015-9482-1
47. Kato F, Miura G, Shirato S, Sato E, Yamamoto S (2015) Correlation between N2 amplitude of multifocal ERGs and retinal sensitivity and retinal nerve fiber layer thickness in glaucomatous eyes. Doc Ophthalmol 131(3):197–206. doi:10.1007/s10633-015-9519-5
48. Todorova MG, Palmowski-Wolfe AM (2011) MfERG responses to long-duration white stimuli in glaucoma patients. Doc Ophthalmol 122(2):87–97. doi:10.1007/s10633-011-9263-4